Journal of NeuroVirology, 14: 205–217, 2008

ISSN: 1355-0284 print / 1538-2443 online
DOI: 10.1080/13550280802008305

informa
healthcare

Differential transcription of matrix-metalloproteinase genes in primary mouse astrocytes and microglia infected with Theiler's murine encephalomyelitis virus

Jirawat Kumnok,[1] Reiner Ulrich,[1] Konstantin Wewetzer,[1,2] Karl Rohn,[3] Florian Hansmann,[1] Wolfgang Baumgärtner,[1] and Susanne Alldinger[1]

[1]Department of Pathology, University of Veterinary Medicine, Hannover, Germany; [2]Center of Anatomy, Hannover Medical School, Hannover, Germany; and [3]Department of Biometry, Epidemiology and Information Processing, University of Veterinary Medicine, Hannover, Germany

The BeAn strain of Theiler's murine encephalomyelitis virus (TMEV) induces demyelinating disease in susceptible mice comparable to human multiple sclerosis. Recent *in vivo* studies showed that matrix metalloproteinases (MMPs) and their inhibitors (tissue inhibitors of MMPs, TIMPs) are associated with demyelination in Theiler's murine encephalomyelitis. The present study was performed to evaluate the *in vitro* MMP and TIMP expression in astrocytes and microglia following TMEV infection. Brain cell cultures from SJL/J mice were infected with the BeAn strain of TMEV and the expressions of 11 MMPs and 4 TIMPs were evaluated by reverse-transcription quantitative polymerase chain reaction (RT-qPCR) at different time points post infection (p.i.). In control astrocytes and microglia, a constitutive expression of MMP-2, -3, -9, -10, -12, -13, -14, -15, -24 and TIMP-2 to -4 was detected. In addition, TIMP-1 and MMP-11 was found in astrocytes only, and MMP-7 was absent in both cells cultures. RT-qPCR demonstrated high virus RNA copy numbers in astrocytes and a low amount in microglia. In accordance, TMEV antigen was detected in astrocytes, whereas it was below the limit of detection in microglia. MMP-3, -9, -10, -12, and -13 as well as TIMP-1 were the enzymes most prominently up-regulated in TMEV-infected astrocytes. In contrast, TMEV infection was associated with a down-regulation of MMPs and TIMPs in microglia. Conclusively, in addition to inflammatory infiltrates, TMEV-induced astrocytic MMPs might trigger a proteolysis cascade leading to an opening of the blood-brain barrier and demyelination *in vivo.* *Journal of NeuroVirology* (2008) **14, 205–217.**

Keywords: brain cell culture; mouse; MMPs; TIMPs; TMEV

Introduction

Theiler's murine encephalomyelitis virus (TMEV), a cardiovirus of the Picornaviridae family (Theiler, 1934), induces a demyelinating encephalomyelitis (Theiler's murine emcephalomyelitis, TME) depending on the virus strain used and the mouse strain infected (Lipton, 1975). TME is a relevant model for the chronic progressive form of human multiple sclerosis (MS; Stohlman and Hinton, 2001; Welsh *et al*, 1990).

Address correspondence to Prof. Dr. Wolfgang Baumgärtner, PhD, Dipl. ECVP, Department of Pathology, University of Veterinary Medicine, Bünteweg 17, 30559 Hannover, Germany. E-mail: wolfgang.baumgaertner@tiho-hannover.de

Jirawat Kumnok and Reiner Ulrich contributed equally to this work.

This article is in memory of Jirawat Kumnok, a young outstanding scientist who passed away far too early.

The authors wish to thank Danuta Waschke and Julia Schirrmeier for excellent technical assistance. Jirawat Kumnok was funded by a grant of the Mahanakorn University, Bangkok, Thailand.

Received 30 November 2007; revised 17 January 2008; accepted 13 February 2008.

In vivo and *in vitro* studies revealed that TMEV can be found in astrocytes, macrophages, microglia, and oligodendrocytes. However, the cellular tropism of TMEV seems to differ depending on the virus strain and the detection system used (Aubert *et al*, 1987; Lipton *et al*, 1995; Oleszak *et al*, 2004; Tsunoda *et al*, 1996; Zheng *et al*, 2001; Zoecklein *et al*, 2003). In BeAn-infected SJL/J mice, TMEV antigen was mainly detected in macrophages, and to a lesser extend, in oligodendrocytes and astrocytes (Dal Canto and Lipton, 1982; Lipton *et al*, 1995). In contrast, in SJL/J mice infected with the DA strain, viral RNA was more often found in oligodendrocytes, astrocytes, and to a lesser extend in microglia/macrophages (Aubert *et al*, 1987). Furthermore, 100 times more viral RNA and 4 times more viral antigen-positive cells were noticed in DA-infected mice compared to BeAn-infected mice (Zoecklein *et al*, 2003). The induction of the innate immune response by TMEV and other Picornaviruses seems to be mediated by multiple cytoplasmic double-stranded RNA (dsRNA)-sensor proteins such as melanoma differentiation-associated gene-5 (Gitlin *et al*, 2006), protein kinase R (Carpentier and Williams, 2007), as well as endosomal Toll-like receptor 3 (So *et al*, 2006). TMEV infection of primary astrocytes leads to the induction of type I interferons and other proinflammatory chemokine and cytokine genes (So *et al*, 2006; Carpentier and Williams, 2007), most likely via the nuclear factor (NF)-κB pathway (Palma *et al*, 2003; Palma and Kim, 2004).

Rubio and Martin-Clemente (1999) found that TMEV was quickly internalized in mouse brain astrocytes and actively replicated in the cytoplasm. c-fos expression peaked 30 min post infection (p.i.) and disappeared 2 h.p.i. and was directly virus induced. Studies with astrocytes originating from mice susceptible and resistant to demyelination showed that following TMEV infection, macrophage inflammatory protein (MIP)-2 chemokine was only induced in astrocytes from genetically susceptible mice (Rubio *et al*, 2006). Interleukin (IL)-1 gene expression is restricted to astrocytes originating from susceptible mouse strains after TMEV infection (Rubio and Capa, 1993).

Mun-Bryce *et al* (2002) found that matrix metalloproteinases (MMPs) are up-regulated prior to the induction of cytokines such as tumor necrosis factor (TNF)-α after lipopolysaccharide (LPS)-induced neuroinflammation. MMPs are enzymes degrading extracellular matrix (ECM) molecules (Matrisian, 1990; Stamenkovic, 2003; Woessner, 1991). According to their substrate specificity, they are categorized into collagenases (MMP-1, -8, -13), gelatinases (MMP-2, -9), stromelysins (MMP-3, -10, -11) including matrilysin (MMP-7), and membrane-type MMPs (MMP-14, -15, -16, -17, -24). MMP-12 or metalloelastase does not belong to a specific group (Massova *et al*, 1998; McCawley and Matrisian, 2001; Yong *et al*, 1998). Activity of MMPs is under control of tissue inhibitors of MMPs (TIMPs; Brew *et al*, 2000). MMPs are of importance for the development of demyelinating diseases as they open the blood-brain barrier, favor invasion and migration of inflammatory cells, trigger the release of TNF-α, and decompose myelin proteins (Baker *et al*, 2002; Ries and Petrides, 1995; Rosenberg *et al*, 1995). Association of MMPs with demyelinating diseases has been shown for MS (Cuzner and Opdenakker, 1999; Hartung and Kieseier, 2000; Leppert *et al*, 2001; Lindberg *et al*, 2001; Rosenberg, 2001, 2002, 2005), TME (Ulrich *et al*, 2006), experimental allergic encephalomyelitis (EAE; Toft-Hansen *et al*, 2004), canine distemper encephalomyelitis (Alldinger *et al*, 2006; Gröters *et al*, 2005; Miao *et al*, 2003), and mouse hepatitis virus (MHV) JHM strain (JHMV) infection of mice (Zhou *et al*, 2002, 2005). Recently, it was shown, that MMP-3 was significantly up-regulated 1 day p.i. (d.p.i.) and in the demyelinating phase of TMEV infection (28 to 196 d.p.i.). MMP-12 mRNA was prominently up-regulated in the demyelinating phase of infection and MMP-12 protein was present in intralesional microglia/macrophages and astrocytes. TIMP-1 mRNA was significantly elevated throughout the observation period (1 to 196 d.p.i.; Ulrich *et al*, 2006). Based on these findings the aim of this study was to determine the role of astrocytes and microglia as a source of MMPs and TIMPs following TMEV infection.

Results

TMEV infection of astrocytes and microglia

TMEV-infected astrocytes formed a confluent monolayer of viable cells throughout the studied time period. Control astrocytes displayed a flat polygonal shape, whereas in infected cultures astrocytes were enlarged consisting of prominent somata and processes. In addition, a mild to moderate cytopathic effect (CPE) consisting of round and detached cells (Figure 1) was noticed. TMEV protein was detected as early as 6 h.p.i. in the cytoplasm of glial fibrillary acidic protein (GFAP)-positive astrocytes. The percentage of TMEV antigen–positive cells increased from 2.0% $\pm$ 2.4% (6 h.p.i.) to 13.1% $\pm$ 6.5% and 13.1% $\pm$ 10.4% (48 and 72 h.p.i.) and decreased to 2.1% $\pm$ 3.7% 240 h.p.i. (Figure 2). Infectious virus was present throughout the observation period and dramatically increased from 8×10^2 plaque-forming units (PFU)/ml at 6 h.p.i. to 3.3×10^5 PFU/ml at 48 h.p.i. (Figure 2). TMEV RNA was first detected 6 h.p.i. and peaked 48 h.p.i. and was present until 240 h.p.i. (Figure 3A).

Control microglia cultures showed a mixed population of ameboid and resting microglia, whereas infected cultures mainly consisted of activated (phagocytic) microglia and single resting forms. Following infection, only a minimal brief transient CPE characterized by increased necrotic detached cells was observed; however, the total number of cells prominently declined towards 240 h.p.i. Virus protein

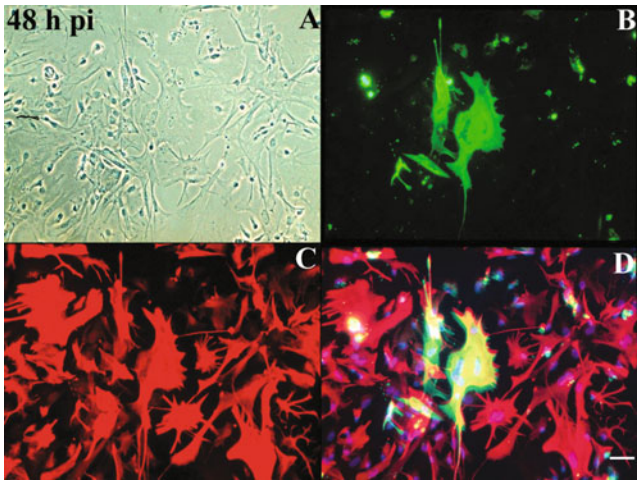

Figure 1 Primary mouse astrocytes infected with the BeAn strain of TMEV at 48 hours post infection (h.p.i.). Infected astrocytes are hypertrophic with an enlarged soma and an increased length of processes and with minimal cytopathic effect consisting of round and detached cells. (**A**) Phase-contrast microscopy; (**B**) green fluorescing TMEV antigen–positive cells (Cy2); (**C**) Red fluorescing GFAP-positive cells (Cy3); (**D**) Overlay of **A** and **B** (Cy2, Cy3, and blue fluorescing nuclei stained with bisbenzimide 0.01%). Scale bar = 6 μm; immunocytochemistry.

could not be detected in the infected microglia cell cultures by immunofluorescence at any time point. In contrast, TMEV RNA was firstly detected and peaking at 6 h.p.i. followed by a prominent decline at 240 h.p.i. (Figure 3B). In comparison, astrocytes displayed approximately 1000 to 10000 higher absolute copy numbers of TMEV RNA than microglia (Figure 3A and B).

MMP and TIMP transcripts

Uninfected astrocytes (day 0, controls) showed a high expression of MMP-2, -11, -14, -15, TIMP-2, -3, and -4. MMP-3, -9, -10, -12, and -24 were moderately expressed and MMP-13 and TIMP-1 showed a low

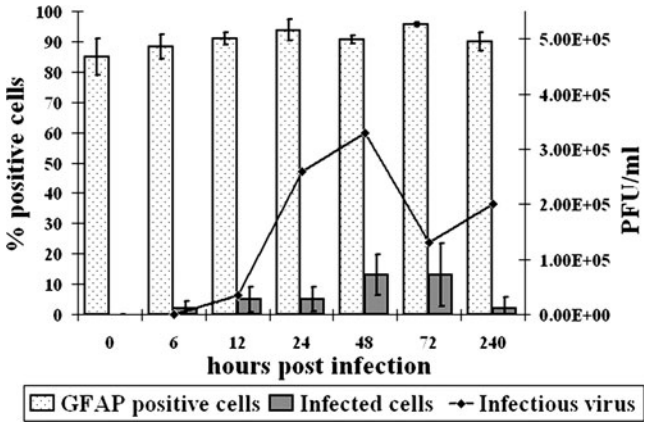

Figure 2 Percentage of GFAP-positive cells (*dot bar*) and infected cells (*grey bar*) on the left *y*-axis (mean ± standard deviation) as determined by immunocytochemistry. The black line displays infectious virus on the right *y*-axis as determined by plaque assays.

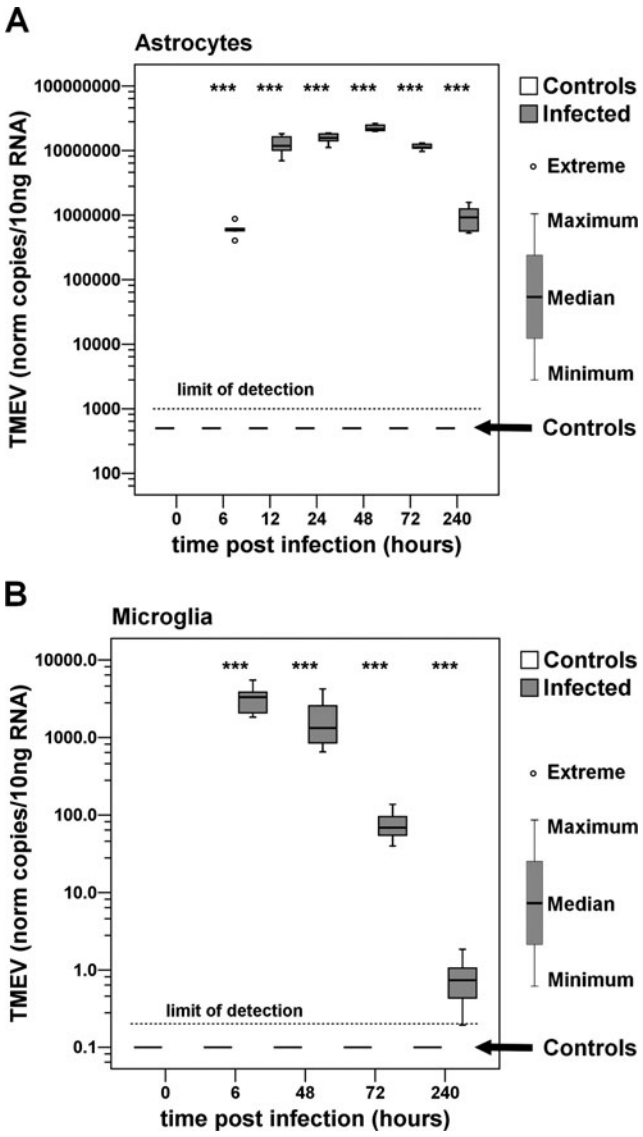

Figure 3 Theiler's murine encephalomyelitis virus (TMEV) RNA transcripts measured by reverse transcriptase–quantitative polymerase chain reaction (RT-qPCR) in astrocytes and microglia. Box and whisker plots exhibit the median and quartiles of normalized copy numbers per 10 ng RNA. Extreme values are shown as circles. (**A**) In astrocytes, TMEV RNA was first detected at 6 h post infection (h.p.i.), peaked at 48 h.p.i. and declined at 240 h.p.i. (**B**) In microglia, TMEV RNA was first detected and peaked at 6 h.p.i. and prominently declined until 240 h.p.i. A significant difference between groups as detected by two-way ANOVA with *post hoc* independent *t* tests is marked as follows: $^{***}p \leq .001$.

expression. MMP-7 was absent (Figure 4A). Noninfected microglia (day 0, controls) showed a high expression of MMP-9, -12, -14, and TIMP-2. MMP-2, -3, -10, -13, -15, -24, and TIMP-4 were moderately expressed and TIMP-3 transcripts were only found in low amounts. MMP-7, -11, and TIMP-1 transcripts were not detected (Figure 4B).

In infected astrocyte cultures, MMP and TIMP mRNAs varied for individual proteins and time points. The MMPs/TIMPs most prominently and

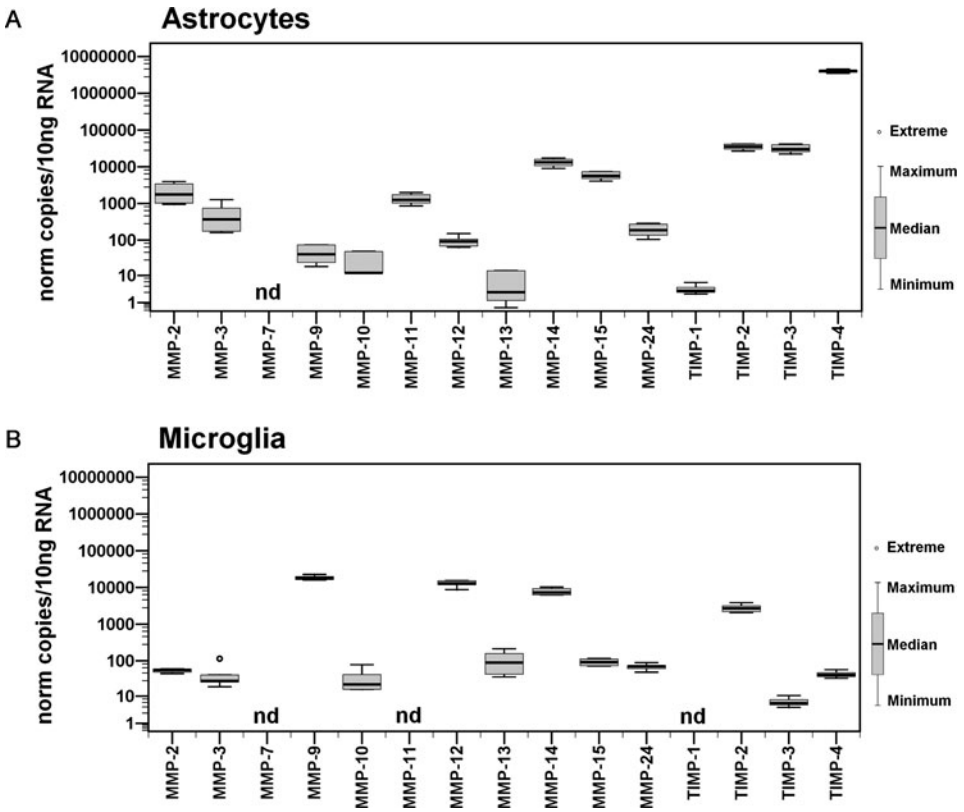

Figure 4 Constitutive expression of MMP and TIMP transcripts in cultured astrocytes and microglia. (**A**) Astrocytes: High expression of MMP-2, -11, -14, -15, TIMP-2, -3, and -4. Moderate expression of MMP-3-, -9, -10, -12, and -24. Low expression of MMP-13 and TIMP-1. MMP-7 transcripts are absent. (**B**) Microglia: High expression of MMP-9, -12, -14, and TIMP-2. Moderate expression of MMP-2, -3, -10, -13, -15, -24, and TIMP-4. Low expression of TIMP-3. MMP-7, -11, and TIMP-1 expression was not detected. Norm = normalized; nd = not detected.

significantly affected by TMEV infection were MMP-3, -9, -10, -12, -13, and TIMP-1. Minor significant up- and down-regulations below a 2.0-fold change in infected compared to controls were observed for MMP-11, -14, -15, -24 and TIMP-3 and -4. Enzymes not significantly influenced by TMEV infection at the time points investigated included MMP-2 and TIMP-2. Similar to controls, MMP-7 was not detected. The relative expression of MMPs and TIMPs is summarized as the ratio of the geometric means of TMEV infected versus noninfected astrocytes in Table 1. MMP-3 was highly significantly up-regulated 48 h.p.i., followed by a peak at 72 h.p.i. and a decline at 240 h.p.i. (Figure 5A). MMP-9 was significantly down-regulated at 12 h.p.i. and significantly up-regulated at 48 h.p.i. and peaked at 72 h.p.i. (Figure 5B). The course of MMP-10 regulation was similar to that of MMP-3, showing a highly significant up-regulation 48 and 72 h.p.i. and a moderate up-regulation at 240 h.p.i. (Figure 5C). The significant up-regulation of MMP-12 was present at 48, 72, and 240 h.p.i. (Figure 5D). MMP-13 was the MMP most prominently up-regulated following TMEV infection and was significantly up-regulated as early as 12 h.p.i. Expression peaked at 72 h.p.i. and declined at 240 h.p.i. (Figure 5E). TIMP-1 was moderately significantly up-regulated beginning at 6 h.p.i., with a peak at 72 h.p.i. and a slight decline at 240 h.p.i. (Figure 5F).

In infected microglia cultures, an overall down-regulation of MMP and TIMP transcripts was observed. The relative expression of MMPs and TIMPs is summarized as the ratio of the geometric means of TMEV infected versus noninfected microglia in Table 2. MMPs/TIMPs displaying moderate (0.5- to 0.1-fold) down-regulations following TMEV infection were MMP-3, -9, -10, -11, -12, -24 and TIMP-2, and -3.

Though the recombinant murine MMP-3, -9, and -12 positive controls were readily detected in the Western blots, no MMP proteins were found in the concentrated supernatants of both astrocyte and microglia cell cultures.

Correlation between TMEV, MMP, and TIMP expressions in astrocyte cultures

The amount of viral RNA as measured by reverse-transcription quantitative polymerase chain reaction (RT-qPCR) and infectious virus expressed as PFU/ml showed a marked significant positive linear correlation ($r = .865$, $p < .001$). TMEV RNA expression was most prominently positively correlated to MMP-13

Table 1 Relative MMP and TIMP expressions during the time course of TMEV infection of astrocytes.

	Hours post infection					
Gene	6	12	24	48	72	240
MMP-2	1.34 (0.77–2.35)[$]	0.98 (0.52–1.85)	0.88 (0.41–1.86)	1.07 (0.5–2.27)	1.05 (0.55–2.01)	1.55 (0.86–2.78)
MMP-3	1.25 (0.72–2.17)	1.11 (0.68–1.8)	1.17 (0.71–1.9)	4.75*** (2.47–9.13)	32.17*** (14.43–71.72)	11.84*** (6.0–23.38)
MMP7	Not detected	Not detected	Not detected	Not detected	Not detected	Not detected
MMP-9	1.25 (0.84–1.86)	0.5** (0.33–0.76)	0.63 (0.38–1.06)	2.96** (1.59–5.5)	11.66*** (6.9–19.71)	1.08 (0.6–1.93)
MMP-10	1.88 (0.61–5.86)	1.44 (0.63–3.27)	1.58 (0.9–2.76)	12.75*** (6.33–25.7)	33.26*** (19.89–55.6)	2.55* (1.14–5.69)
MMP-11	1.26 (0.81–1.98)	0.9 (0.67–1.2)	0.8* (0.67–0.96)	0.56*** (0.44–0.71)	0.39*** (0.29–0.52)	1.12 (0.92–1.36)
MMP-12	0.85 (0.53–1.37)	1.18 (0.88–1.57)	1.01 (0.6–1.64)	1.83* (1.0–3.35)	17.53*** (11.26–27.27)	7.26*** (5.2–10.14)
MMP-13	0.79 (0.37–1.66)	1.85** (1.25–2.74)	4.74*** (2.67–8.43)	45.51*** (9.43–219.53)	116.68*** (51.35–265.08)	11.56*** (4.95–26.99)
MMP-14	1.4* (1.04–1.88)	1.11 (0.91–1.36)	1.01 (0.78–1.31)	1.19 (0.95–1.48)	1.16 (0.99–1.36)	1.32 (0.96–1.81)
MMP-15	0.94 (0.71–1.24)	1.17 (0.97–1.41)	0.93 (0.81–1.07)	0.76** (0.64–0.91)	0.28*** (0.2–0.39)	0.68** (0.54–0.87)
MMP-24	1.08 (0.7–1.65)	0.61* (0.4–0.95)	0.98 (0.71—1.35)	1.42* (1.0–2.01)	1.03 (0.67–1.57)	0.22*** (0.17–0.3)
TIMP-1	1.53* (1.05–2.24)	1.69* (1.13–2.54)	1.47 (0.99–2.2)	4.07*** (2.52–6.59)	10.66*** (7.7–14.75)	7.97*** (3.69–17.21)
TIMP-2	1.26 (0.76–2.1)	1.13 (0.7–1.85)	1.05 (0.72—1.55)	1.1 (0.7–1.72)	0.75 (0.55–1.02)	0.94 (0.67–1.32)
TIMP-3	1.75*** (1.4–2.2)	1.23* (1.04–1.44)	1.04 (0.92—1.17)	1.49** (1.19–1.87)	1.08 (0.91–1.28)	1.43*** (1.25–1.63)
TIMP-4	1.02 (0.72–1.43)	1.12 (0.88–1.42)	1.14 (0.75—1.72)	0.68* (0.48–0.96)	0.33*** (0.26–0.41)	0.45** (0.29–0.68)

Note. Values show the ratio of the geometric means of normalized copy numbers/10 ng RNA from infected versus control astrocytes, with the upper and the lower limits of the 95% confidence interval. Moderate (2- to 10-fold) up-regulations are marked in light gray, severe (>10 fold) up-regulations in dark grey. Significant difference of the ratio from one as revealed by two-way ANOVA with *post hoc* independent *t* tests is marked as follows: * $p \leq .05$; ** $p \leq .01$; *** $p \leq .001$.
[$]Lower to upper limits of the 95% confidence interval.

($r = .673$; $p < .001$) and TIMP-1 ($r = .662$, $p < .001$). Moderate positive correlations were calculated for TMEV RNA and MMP-3 (0.522, $p < .001$), MMP-10 (0.582, $p < .001$), and TIMP-3 ($r = 0.568$, $p < .001$). Further minor significant positive correlations were found for TMEV RNA and MMP-12 ($r = 0.377$, $p < .001$) and MMP-14 ($r = 0.389$, $p < .001$). MMP-11, -15, and TIMP-4 showed minor significant negative correlations to TMEV RNA ($r = -.398$, $p < .001$; $r = -.291$, $p = .010$; $r = -.327$, $p = .003$). MMP-13 was the only enzyme showing a moderate significant positive correlation to the amount of infectious virus ($r = 0.552$; $p < .05$).

Discussion

In this study the presence of transcripts of 11 MMPs and 4 TIMPs was evaluated in primary mouse astrocytes and microglia at different time points following infection with the BeAn strain of TMEV. Infected astrocytes showed an increased transcription of MMP and TIMP genes including most prominently MMP-3, -9, -10, -12, -13, and TIMP-1. Additionally, infected astrocytes displayed a mild to moderate cytopathic effect characterized by single-cell necrosis and infectious virus was retrieved throughout the observation period. The reduced detection of infectious virus at 6 h.p.i. by using the plaque assay compared to the detection of viral RNA by RT-qPCR is most likely related to the early stage of the virus replication cycle, which lasts for 5 to 10 h for Picornaviridae (Racaniello, 2001). During this stage, viral RNA but not progeny virus can be detected easily. In addition, TMEV antigen was readily detected in infected cultures, indicating viral replication and viral protein synthesis. Astrocytes allowed TMEV BeAn to replicate at a higher rate compared to microglia, as reported previously in *in vitro* studies (Zheng *et al*, 2001). Microglia exhibited a restricted TMEV infection and allowed virus replication on a low level only. According to Oleszak *et al* (2004), the susceptibility of microglia to TMEV infection is different from macrophages, and blood-borne activated macrophages represent the main cell type responsible for viral persistence within the lesions. Accordingly, *in vitro* studies showed that TMEV preferentially infects activated macrophages (Jelachich *et al*, 1999). Interestingly, delayed apoptosis of macrophages is a well-known feature of such an infection (Lipton *et al*,

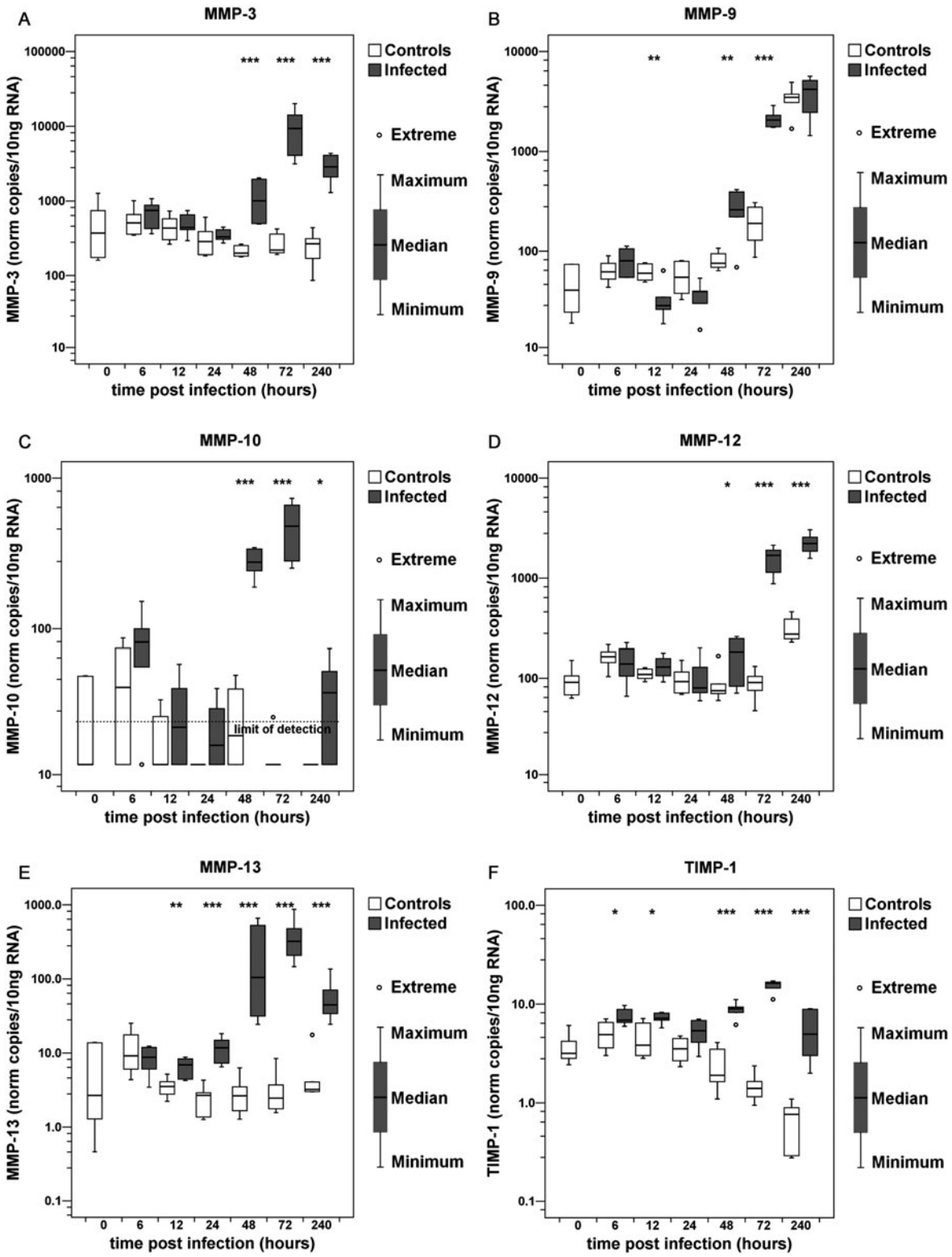

Figure 5 Matrix metalloproteinase (MMP)-3, -9, -10, -12, -13, and tissue inhibitor of metalloproteinase (TIMP)-1 transcripts in cultured astrocytes as measured by reverse transcriptase–quantitative polymerase chain reaction (RT-qPCR). Box and whisker plots show the median and quartiles of normalized copies/10 ng RNA. Extreme values are shown as circles. (**A**) Moderate up-regulation of MMP-3 mRNA at 48 h post infection (h.p.i.), peaking at 72 h.p.i. and declining at 240 h.p.i. in infected cultures compared to controls. (**B**) Moderate down-regulation of MMP-9 mRNA at 12 h.p.i. and moderate up-regulation at 48 and 72 h.p.i. (**C**) A severe up-regulation of MMP-10 at 48 and 72 h.p.i. (**D**) Marked up-regulation of MMP-12 at 48, 72, and 240 h.p.i. (**E**) Significant up-regulation of MMP-13 from 24 to 240 h.p.i., peaking at 72 h.p.i. (**F**) Moderate up-regulation of TIMP-1 beginning from 48 h.p.i., peaking at 72 h.p.i. and slightly declining at 240 h.p.i. in infected cultures compared to controls. A significant difference between the groups as detected by two-way ANOVA with *post hoc* independent *t* tests is marked as follows: $^{*}p \leq .05$; $^{**}p \leq .01$; $^{***}p \leq .001$.

Table 2 Relative MMP and TIMP expressions during the time course of TMEV infection of microglia.

	Hours post infection			
Gene	6	48	72	240
MMP-2	1.53 (0.91—2.55)[$]	1.48* (1.10–2.00)	1.30 (0.97–1.75)	0.70* (0.53–0.93)
MMP-3	0.93 (0.56–1.57)	0.20*** (0.10–0.40)	0.38** (0.23–0.64)	0.357** (0.19–.67)
MMP7	Not detected	Not detected	Not detected	Not detected
MMP-9	0.50*** (0.39–0.65)	0.31*** (0.23–0.43)	0.33*** (0.24–0.45)	0.56*** (0.43–0.72)
MMP-10	1.29 (0.72–2.31)	0.40*** (0.29–0.56)	0.73 (0.49–1.07)	0.80 (0.55–1.15)
MMP-11	Not detected	1.00 (0.37–2.69)	2.03 (0.68–6.01)	0.38* (0.16–0.92)
MMP-12	1.05 (0.77–1.41)	0.51*** (0.42–0.61)	0.76* (0.60–0.95)	0.20*** (0.16–0.26)
MMP-13	4.62*** (3.14–6.78)	0.61* (0.39–0.94)	0.91 (0.60–1.39)	0.41 (0.12–1.37)
MMP-14	0.81 (0.61–1.07)	1.63*** (1.31–2.03)	1.10 (0.81–1.51)	0.68*** (0.57–0.81)
MMP-15	0.62** (0.47–0.82)	0.94 (0.67–1.34)	1.52* (1.03–2.25)	0.61 (0.33–1.15)
MMP-24	0.67* (0.49–0.93)	1.02 (0.74–1.39)	0.82 (0.53–1.28)	0.18*** (0.09–0.39)
TIMP-1	Not detected	Not detected	1.33 (0.64–2.77)	Not detected
TIMP-2	0.79* (0.64–0.98)	0.85 (0.65–1.10)	0.53*** (0.40–0.71)	0.11*** (0.09–0.14)
TIMP-3	0.94 (0.21–4.29)	1.46* (1.05–2.04)	1.21 (0.88–1.66)	0.15*** (0.11–0.22)
TIMP-4	0.83 (0.59–1.18)	1.03 (0.69–1.53)	0.85 (0.58–1.24)	0.18*** (0.10–0.31)

Note. Values show the ratio of the geometric means of normalized copy numbers/10 ng RNA from infected versus control microglia, with the upper and the lower limits of the 95% confidence interval. Moderate (0.5- to 0.1-fold) down-regulations are marked in light gray. Significant difference of the ratio from one as revealed by two-way ANOVA with *post hoc* independent *t* tests is marked as follows: * $p \leq .05$; ** $p \leq .01$; *** $p \leq .001$.
[$]Lower to upper limits of the 95% confidence interval.

2005). This delayed apoptosis might also occur in virus-infected microglia and is accompanied by interrupted host protein synthesis and thus results in a down-regulation of MMPs and TIMPs in microglia as seen in the present study.

Constitutive MMP and TIMP expression in noninfected astrocyte and microglia cell cultures

MMP-2, -3, -9, -10, -11, -12, -13, -14, -15, and -24 mRNAs were constitutively expressed in control astrocyte cultures, whereas MMP-7 was absent. In addition, all four known TIMPs were present in control astrocytes. The observed expression profile of astrocytes and microglia is in accordance with previous findings (Crocker *et al*, 2006; Gottschall *et al*, 1995; Liuzzi *et al*, 2004). Similarly, MMP-12 is among the most highly expressed genes in microglia and the total copy number is approximately 100-fold higher than in astrocytes.

MMP and TIMP expression of BeAn-infected astrocyte and microglial cell cultures

In the present study, infection of primary astrocytes from SJL/J mice with the BeAn strain of TMEV induced increased transcription of MMP and TIMP genes, including most prominently MMP-3, -9, -10, -12, -13, and TIMP-1. Minor significant changes were found for MMP-11, -14, -15, -24 and TIMP-3 and -4. Enzymes not significantly influenced by TMEV infection included MMP-2, -7, and TIMP-2. Though a high degree of purity of enriched astrocyte cultures was obtained, a contributing role of few contaminating other glial cells, especially microglia, as a potential source of the observed MMP and TIMP up-regulation cannot be ruled out. Subsequently, isolated and infected microglia were investigated for MMP and TIMP expression. However, in contrast to astrocytes, TMEV infection of microglia resulted in an overall down-regulation of MMP and TIMP transcripts.

MMP-2 transcripts were not significantly changed after TMEV infection of astrocytes. This finding parallels the results of an *in vivo* study (Ulrich *et al*, 2006). In MS, however, MMP-2 up-regulation seems to be associated with the early events in plaque formation (Lindberg *et al*, 2001).

MMP-3 gene expression was significantly up-regulated in infected astrocytes as early as 48 h.p.i. and until the end of the observation period at 240 h.p.i. Similarly, in an *in vivo* study evaluating MMP and TIMP gene expression following TMEV BeAn infection of SJL/J mice, MMP-3 was found to be significantly up-regulated on 1 d.p.i. and from 28 to 196 d.p.i. (Ulrich *et al*, 2006), although the transferability of the *in vitro* situation to the more complex *in vivo* situation remains unknown. Interestingly, in coronavirus infection of mice, another viral model for MS, increased MMP-3 expression seemed to be restricted to astrocytes (Zhou *et al*, 2005). In acute and subacute demyelinating canine distemper encephalitis, MMP-3 proteins, together with MMP-1, -7, -9, -12, -13, and -14, were present in astrocytes and microglia/macrophages (Miao *et al*, 2003). In MS, MMP-3 mRNA transcripts were up-regulated in early lesions characterized by an inflammatory edema of myelin sheaths; however, overt demyelination was not observed (Lindberg *et al*, 2001).

In infected astrocytes, MMP-9 displayed an increased expression pattern similar to MMP-3 at 48 and 72 h.p.i.; however, there was no significant difference compared to controls at 240 h.p.i. In contrast, MMP-9 belonged to the genes significantly down-regulated in infected microglial cultures and seemed not to be affected by TMEV BeAn infection *in vivo* (Ulrich *et al*, 2006). This difference might be explained by the absence of immune cell–mediated signals following virus-infection *in vitro*. MMP-9 activity and protein expression is inhibited by interferon-β (IFN-β) and -γ (Ma *et al*, 2001). Decreased MMP-9 mRNA levels and suppressed MMP-9

promoter activity are dependent on the transcription factor STAT-1α (Ma *et al*, 2001). Interestingly, in *in vivo* studies, IFN-γ gene expression is significantly up-regulated following TMEV BeAn infection (Gerhauser *et al*, 2007b) and, as expected, it is absent in TMEV BeAn–infected astrocytes (Gerhauser *et al*, unpublished observation). In MS, MMP-9 is up-regulated (Cossins *et al*, 1997; Lindberg *et al*, 2001) and is believed to be a key element in the blood-brain barrier breakdown (Rosenberg *et al*, 1995; Rosenberg, 2002). In mice with EAE, contradictory results have been obtained concerning MMP-9 expression (Clements *et al*, 1997; Pagenstecher *et al*, 1998; Teesalu *et al*, 2001; Toft-Hansen *et al*, 2004).

Another significantly up-regulated MMP after TMEV BeAn infection of astrocytes was MMP-10. This enzyme is among the most prominently up-regulated MMPs and TIMPs in EAE, another model for MS (Toft-Hansen *et al*, 2004). In this study, MMP-10 expression was associated with cells forming perivascular cuffs. A strong MMP-10 expression has further been observed in neoplastic gemistocytic astrocytes and seems to be related to a worse prognosis of astrocytic tumours compared to oligodendrogliomas (Thorns *et al*, 2003). MMP-10 up-regulation might thus be a stereotypical sign of astrocytic activation following various insults.

In infected astrocytes, MMP-12 expression was significantly up-regulated 24 h later than the other MMPs and TIMP-1. *In vivo*, MMP-12 was the enzyme most prominently up-regulated in the demyelinating phase of TME (Ulrich *et al*, 2006). Although MMP-12 expression is up-regulated in astrocytes following TMEV infection, it remains unaltered or moderately down-regulated in microglia. Still, the absolute amount of MMP-12 mRNA in microglia cultures was higher than in astrocyte cultures. Because it is unclear wheter the *in vitro* situation is directly transferable to the more complex *in vivo* situation, the previously reported up-regulation of MMP-12 in the spinal cord in the late phase of TME can be the result of (a) an up-regulation of MMP-12 transcription in reactive astrocytes and (b) an increase in the number of microglia and macrophages or (c) a combination of both. In addition, it still remains a possibility that microglia cocultured with other brain cells including astrocytes might respond differently to TMEV infection compared to single-cell cultures. A stimulation of microglial/macrophage MMP-12 expression by other indirectly virus-induced pathways might therefore play an essential role during the *in vivo* pathogenesis of TMEV-induced myelin loss. This is supported by the immunohistochemical demonstration of MMP-12 in astrocytes as well as microglia/macrophages within lesions *in vivo* (Ulrich *et al*, 2006). Furthermore, there is a severely increased number of intralesional microglia/macrophages following TMEV infection of SJL/mice (Gerhauser *et al*, 2007a). MMP-12 or macrophage metalloelastase is able to cleave various molecules including myelin basic protein (MBP; Chandler *et al*, 1996; Gronski *et al*, 1997). In MS and EAE, MMP-12 was present in demyelinating lesions and is suspected to be involved in myelin destruction (Pagenstecher *et al*, 1998; Vos *et al*, 2003). In coronavirus infection of mice, MMP-12 was expressed by central nervous system (CNS) resident cells and inflammatory cells (Zhou *et al*, 2005). In chronic demyelinating distemper encephalitis, the protein of MMP-12 was detected in macrophages, microglia, astrocytes, and perivascular mononuclear infiltrates (Miao *et al*, 2003).

Surprisingly, in infected astrocytes, MMP-13 showed the fastest and most prominent up-regulation post infection. In addition, MMP-13 mRNA was most strikingly positively correlated to TMEV RNA and infectious virus expression. MMP-13 up-regulation is described in demyelinating canine distemper encephalitis, a disease with prominent infection of astrocytes (Miao *et al*, 2003) and in bacterial meningitis (Kieseier *et al*, 1999). Although a robust mesenchymal expression and collagenolytic activity of MMP-13 is known to be a key feature in pathological conditions such as osteoarthritis and rheumatoid arthritis (Im *et al*, 2007; Neuhold *et al*, 2001), the function and contributing role of MMP-13 during neuroinflammatory and neurodegenerative disease remains undetermined and warrants further studies.

The TIMP most significantly affected by TMEV BeAn infection in astrocytes was TIMP-1, whereas its expression was below the detection limit in microglia and remained unchanged after infection. *In vivo,* TIMP-1 mRNA was significantly up-regulated in the acute and chronic disease (Ulrich *et al*, 2006). Although the transferability of the *in vitro* situation to the more complex *in vivo* situation is unclear, up-regulation of TIMP-1 represents a well-known response of astrocytes to injury (Jaworski, 2000). However, TIMP-1 protein was mainly found in CD4+ lymphocytes and not in astrocytes and CD8+ cells in coronavirus infection of mice (Zhou *et al*, 2005).

In summary, the present study shows that TMEV BeAn infection of astrocytes induced increased transcription of MMP-3, -9, -10, -12, -13, and TIMP-1. In contrast, TMEV infection of microglia resulted in an overall down-regulation of MMP and TIMP transcripts. Thus, enhanced transcription of proteolytic enzymes following TMEV infection of astrocytes might be the initial event in proteolysis observed in demyelinating diseases and astrocytes might be the key cells triggering processes leading to demyelination. However, the complex interactions between astrocytes, microglia and TMEV need to be investigated in detail in further studies.

Materials and methods

Animals

Adult SJL/J mice were purchased from Harlan Winkelmann (Borchen, Germany) and maintained

in a microisolator cage system (Tecniplast, Hohenpeißenberg, Germany) for breeding. One- to 3-day-old pups were used for cell isolation. Breeding and killing of animals was authorized by the ethical commission of the Landeshauptstadt Hannover (permission number 42500/1H).

Astrocyte and microglia cultures

Mixed glial cell cultures were established from cerebral hemispheres of 1- to 3-day-old mice according to McCarthy and deVellis (1989) and Giulian and Baker (1986). Briefly, cerebral cortices were isolated under a dissecting microscope and cleaned of meninges followed by mechanical dissociation in calcium-free phosphate-buffered (PBS), pH 7.4, containing 0.8 g/L Na-EDTA, 2 mg/ml trypsin, and 0.2 mg/ml DNase I (Roche Diagnostics, Mannheim, Germany) and incubation at 37°C for 20 min. After centrifugation at 250 × *g* at 4°C for 10 min, cell pellets were resuspended in defined Sato's medium (Bottenstein and Sato, 1979), supplemented with 10% fetal calf serum (FCS), and cells were singulated using a fire-polished Pasteur pipette. Cells (5×10^6) were seeded on poly-L-lysine (100 μg/ml)–coated 75-ml flasks (Nunc, Wiesbaden, Germany). Cultures were maintained in Sato's medium–10% FCS under standard conditions (5% CO_2, 37°C) and medium was changed 24 h, 72 h, and 6 days after seeding.

Seven days after seeding, the cells reached confluency. Flasks were sealed with Parafilm and microglia were separated by shaking at 37°C, 150 rpm, on a rotary platform shaker (Innova 2000; New Brunswick Scientific, New Jersey, USA) for 45 min. The flasks were then washed twice and the remaining cells were cultured in Sato's medium −10% FCS for at least 4 h. Then the flasks were agitated twice overnight to remove oligodendrocyte precursor cells. The flasks were sealed with Parafilm and shaken at 200 rpm, 37°C, on a rotary platform shaker. The remaining astrocyte cultures reproducibly displayed a purity of 90% to 95%. The remaining cells included few fibroblasts and other glial cells like microglia. Microglia cultures were 97% pure. The enriched astrocytes and microglia were seeded onto 24-well plates (Costar; Corning, Germany; 1×10^5 cells/well) and cultured in Sato's medium −10% FCS. For microglia, the medium was supplemented with macrophage colony-stimulating factor (M-CSF; 40 ng/ml). The medium was changed every second day. The experiment started 24 h after seeding. Quantification of cells was performed by counting five different high-power fields in one coverslip preparation.

Immunofluorescence and controls

TMEV was visualized by using a mouse monoclonal antibody directed against VP1 of the DA strain of TMEV diluted 1:100 (DAmAb2, kindly provided by Prof. Raymond P. Roos, Department of of Neurology, University of Chicago Medical Center, Chicago Illinois). Astrocytes were identified using a polyclonal rabbit anti-glial fibrillary acidic protein (GFAP) antibody (Dako Cytomation, Hamburg, Germany) diluted 1:400. Microglia were identified using a polyclonal rabbit anti-Iba-1 antibody (Wako Chemicals, Neuss, Germany) diluted 1:250 and 1,1′-dioctadecyl-3,3,3′,3′-tetramethylindocarbocyanine perchlorate (DiI-acLDL; Paesel+Lorey, Hanau, Germany). Primary mouse fibroblasts served as negative controls for immunocytochemistry. For double immunostaining, cultures grown on coverslips were washed twice with Sato's medium, followed by PBS and fixed with 4% paraformaldehyde, pH 7.4, for 15 min at room temperature. Primary antibodies were added to PBS containing 5% horse and goat normal serum and 0.25% Triton X-100. Cells were incubated with this solution overnight at 4°C. Secondary antibodies included Cy2-conjugated AffiniPure goat anti-mouse immunoglobulin G (IgG) (H+L) and Cy3-conjugated AffiniPure goat anti-rabbit IgG (H+L; Jackson ImmunoResearch Laboratories, Dianova, Hamburg, Germany) diluted 1:200. Cultures were finally subjected to a nuclear stain with 0.01% bis-benzimide (Sigma-Aldrich, München, Germany) in distilled water 10 min at room temperature. Coverslips were mounted with fluorescent mounting medium (Dako Cytomation) and observed under an inverted microscope (Olympus IX-70; Olympus Optical, Hamburg, Germany). Microphotographs were taken using the PM-30 photo system (Olympus Optical) and a color reversal film ISO400 (Ektachrome 400X EPL135-36; Kodak, Rochester, New York).

Virus and experimental design

The TMEV BeAn 8386 strain was originaly isolated from a feral mouse in Belem, Brazil, in 1957 (Rozhon *et al*, 1983; a gift from Dr. H. L. Lipton, Department of Neurology, Northwestern University Medical School, Chicago, Illinois). It was propagated in baby hamster kidney (BHK)-21 cells (a gift from Prof. Raymond P. Roos) cultured in Dulbecco's modified Eagle's medium (DMEM; PAA Laboratories, Pasching, Germany) supplemented with 10% FCS and 100 U/ml penicillin/100 μg/ml streptomycin. Virus with a titer of 5.5×10^8 PFU/ml was used for the experiments. Cells were infected with TMEV BeAn at a multiplicity of infection (MOI) of 1.0 at 24 h post seeding using 2×10^5 PFU per well. Mock-infected controls received Sato's medium −10% FCS only. Supernatants and total cellular RNA of TMEV-infected astrocyte cultures and controls were harvested 0, 6, 12, 24, 48, 72, and 240 h.p.i. Supernatants and total cellular RNA of TMEV-infected microglia cultures and controls were harvested 0, 6, 48, 72, and 240 h.p.i. Plaque assays were done in duplicates. Briefly, supernatants serially diluted from 10^{-2} to 10^{-6} were used for inoculation of confluent monolayer cultures of murine lung tumor cells (L2 cells; a gift from Prof. C. Jane Welsh, Department of Veterinary Integrative Biosciences, College of Veterinary Medicine and Biomedical Sciences, Texas A&M University, College

Station, Texas) in 6-well plates (Nunc, Wiesbaden, Germany), including 1 well for negative controls. L2 cells were incubated with the serially diluted supernatants for 1 h at room temperature, followed by the application of 0.4% methylcellulose in DMEM with 2% FCS. Plaques were stained with 1% crystal violet after 72 h and the number of plaques was evaluated and expressed as PFU/ml.

RT-qPCR

RNA was isolated from 6-cell culture wells/time point using the RNeasy Mini Kit (Qiagen, Hilden, Germany) according to the manufacturer's instructions as described (Gerhauser *et al*, 2005; Markus *et al*, 2002). RNA concentration was measured at 260 nm employing a spectral photometer (GeneQuant Pro; Amersham Biosciences Europe, Freiburg, Germany) and final RNA concentration was set to 10 ng/μl. RNA was reversely transcribed using the Omniscript Reverse Transcriptase Kit (Qiagen), 10 μM random hexamers (Random Primers; Promega, Mannheim, Germany), and 0.5 U/μl Rnase inhibitor (RNase OUT; Invitrogen, Karlsruhe, Germany). Quantitative polymerase chain reaction (qPCR) was performed with 1 μl cDNA/25 μl reaction with the Brilliant SYBR Green qPCR Core Reagent Kit (Stratagene Europe, Amsterdam, The Netherlands) using the MX3005P^{M} Multiplex Quantitative PCR System (Stratagene) with optimized reaction conditions. Primer pairs specific for TMEV, MMP (-2, -3, -7, -9, -10, -11, -12, -13, -14, -15, -24), TIMP (-1 to -4), and housekeeping gene (GAPDH, HPRT, SDHA, β-actin) RNAs were used (Ulrich *et al*, 2005, 2006). A duplicate log 10 dilution series of cDNA with 10^2 to 10^8 copies/μl was used as external standard for absolute quantification (Gerhauser *et al*, 2005; Ulrich *et al*, 2005, 2006). Multiple murine organs, including uterus, ovary, spleen, kidney, brain, spinal cord, and jejunum, with a known constitutive MMP and TIMP expression were used as positive controls (Khasigow *et al*, 2000; Pagenstecher *et al*, 1998; Rudolph-Owen *et al*, 1997; Ulrich *et al*, 2005, 2006). Furthermore, specificity of the positive reaction was confirmed by melting point analysis.

Astrocytes and microglia were processed and investigated in separate experiments. Data were analyzed employing the MX3005P^{TM} software Version 2.02 (Stratagene). Normalization of data was achieved by geometric averaging of multiple housekeeping genes using the geNorm software Version 3.4 (Vandesompele *et al*, 2002). Accordingly, for astrocytes an internal control gene stability measure (M-value) of 0.552, 0.556, 0.851, and 0.673 was retrieved for GAPDH, HPRT, β-actin, and SDHA, respectively. The applied normalization factor was obtained by geometric averaging the three most stable housekeeping genes, GAPDH, HPRT, and SDHA, for astrocytes. For microglia, a M-value of 0.787, 0.841, 0.810, and 0.869 was retrieved for GAPDH, HPRT, β-actin and SDHA, respectively. The normalization factor for microglia was derived by geometric averaging the three most stable housekeeping genes, GAPDH, HPRT, and β-actin.

Western blots

Western blots for the detection of MMP-3, -9, and -12 proteins were prepared from cell culture supernatants of TMEV-infected as well as control astrocytes and microglia. The cell culture supernatants were approximately 10-fold concentrated employing Vivaspin 500 devices (Sartorius, Goettingen, Germany). Fifteen microliters of the concentrated supernatants were subjected to sodium dodecyl sulfate (SDS)-polyacrylamide gel electrophoresis. One hundred nanograms of recombinant murine MMP-3, -9, and -12 (R&D Systems, Wiesbaden, Germany) were used as positive controls. The separated proteins were transferred to Trans-Blot Transfer Medium (Bio-Rad Laboratories, Munich, Germany) by a tank-blotting system (Carl Roth, Karlsruhe, Germany) at 250 V and 400 mA for 1.5 h. After blocking of nonspecific binding by 5% skim milk powder (Merck, Darmstadt, Germany), the membranes were incubated with either a monoclonal rabbit anti-MMP-3 antibody diluted 1:1000 (Epitomics, Burlingame, USA), a polyclonal rabbit anti-MMP-9 antibody diluted 1:2000 (Abcam, Cambridge, UK), or a polyclonal goat anti-MMP-12 antibody diluted 1:250 (Santa Cruz Biotechnology, Santa Cruz, USA), respectively. After incubation with a horseradish peroxidase–conjugated secondary antibody, protein was visualized using Super Signal West Pico Chemiluminescent Substrate (Pierce, Rockford, USA).

Statistical analysis

Statistical analysis was accomplished using the SPSS for Windows Version 13.0 software package (SPSS). The numbers of immunofluorescence-positive cells are presented as mean and standard deviation. The normalized copy numbers/10 ng RNA obtained from the RT-qPCR were log-transformed prior to statistical analysis. RT-qPCR samples without measurable mRNA (no C_T) were set to detection limit divided by 2. Hereby, detection limit was either the external standard, the positive control, or the sample with the lowest amount of detectable mRNA and a correct melting point. Box and whisker plots were drawn to display the median and the quartiles. Statistical differences were evaluated by using two-way analysis of variance (ANOVA) for the factors group (control or TMEV infected) and time (time post infection) simultaneously with *post hoc* independent *t* tests for the different time points. Pearson's product moment correlation coefficient was calculated to demonstrate the relationship between TMEV RNA/PFU, MMP, and TIMP mRNA expression. Statistical significance was designated as $p \leq .05$.

References

Alldinger S, Gröters S, Miao Q, Fonfara, S, Kremmer, E, Baumgärtner, W (2006). Roles of an extracellular matrix (ECM) receptor and ECM processing enzymes in demyelinating canine distemper encephalitis. *Dtsch tierärztl Wschr* **113:** 151–168.

Aubert C, Chamorro M, Brahic M (1987). Identification of Theiler's virus infected cells in the central nervous system of the mouse during demyelinating disease. *Microb Pathogen* **3:** 319–326.

Baker AH, Edwards DR, Murphy G (2002). Metalloproteinase inhibitors: biological actions and therapeutic opportunities. *J Cell Sci* **115:** 3719–3727.

Bottenstein JE, Sato GH (1979). Growth of a rat neuroblastoma cell line in serum-free supplemented medium. *Proc Natl Acad Sci U S A* **76:** 514–517.

Brahic M (2002). Theiler's virus infection of the mouse, or: of the importance of studying animal models. *Virology* **301:** 1–5.

Brew K, Dinakarpandian D, Nagase H (2000). Tissue inhibitors of metalloproteinases: evolution, structure and function. *Biochim Biophys Acta* 1**477:** 267–283.

Carpentier PA, Williams BR (2007). Distinct roles of protein kinase R and toll-like receptor 3 in the activation of astrocytes by viral stimuli. *Glia* **55:** 239–252.

Chandler S, Cossins J, Lury J, Wells G (1996). Macrophage metalloelastase degrades matrix and myelin proteins and processes a tumour necrosis factor-alpha fusion protein. *Biochem Biophys Res Commun* **228:** 421–429.

Clements JM, Cossins JA, Wells GM, Corkill DJ, Helfrich K, Wood LM, Pigott R, Stabler G, Ward GA, Gearing AJ, Miller KM (1997). Matrix metalloproteinases expression during experimental autoimmune encephalomyelitis and effects of a combined matrix metalloproteinase and tumour necrosis factor-alpha inhibitor. *J Neuroimmunol* **74:** 85–94.

Cossins JA, Clements JM, Ford J, Miller KM, Pigott R, Vos W, van der Valk P, de Groot CJ (1997). Enhanced expression of MMP-7 and MMP-9 in demyelinating multiple sclerosis lesions. *Acta Neuropathol* **94:** 590–598.

Crocker SJ, Milner R, Pham-Mitchell N, Campbell IL (2006). Cell and agonist-specific regulation of genes for matrix metalloproteinases and their tissue inhibitors by primary glial cells. *J Neurochem* **98:** 812–823.

Cuzner ML, Opdenakker G (1999). Plasminogen activators and matrix metalloproteases, mediators of extracellular proteolysis in inflammatory demyelination of the central nervous system. *J Neuroimmunol* **94:** 1–14.

Dal Canto MC, Lipton HL (1982). Ultrastructural immunohistochemical localization of virus in acute and chronic demyelinating Theiler's virus infection. *Am J Pathol* **106:** 20–29.

Gerhauser I, Alldinger S, Baumgärtner W (2007a). Ets-1 represents a pivotal transcription factor for viral clearance, inflammation, and demyelination in a mouse model of multiple sclerosis. *J Neuroimmunol* **188:** 86–94.

Gerhauser I, Alldinger S, Ulrich R, Baumgärtner W (2005). Spatio-temporal expression of immediate early genes in the central nervous system of SJL/J mice. *Int J Dev Neurosci* **23:** 637–649.

Gerhauser I, Ulrich R, Alldinger S, Baumgärtner W (2007b). Induction of activator protein-1 and nuclear factor-κB as a prerequisite for disease development in susceptible SJL/J mice after Theiler murine encephalomyelitis. *J Neuropathol Exp Neurol* **66:** 809–818.

Gitlin L, Barchet W, Gilfillan S, Cella M, Beutler B, Flavell RA, Diamond MS, Colonna M (2006) Essential role of mda-5 in type I IFN responses to polyriboinosinic:polyribocytidylic acid and encephalomyocarditis picornavirus. *Proc Natl Acad Sci U S A* **103:** 8459–8464.

Giulian D, Baker TJ (1986). Characterization of ameboid microglia isolated from developing mammalian brain. *J Neurosci* **6:** 2163–2178.

Gottschall PE, Yu X, Bing B (1995). Increased production of gelatinase B (matrix metalloproteinase-9) and interleukin-6 by activated rat microglia in culture. *J Neurosci Res* **42:** 335–342.

Gronski TJ, Martin RL, Kobayashi DK, Walsh BC, Holman MC, Huber M, Van Wart HE, Shapiro SD (1997). Hydrolysis of a broad spectrum of extracellular matrix proteins by human macrophage elastase. *J Biol Chem* **272:** 12189–12194.

Gröters S, Alldinger S, Baumgärtner W (2005). Upregulation of mRNA for matrix metalloproteinases-9 and -14 in advanced lesions of demyelinating canine distemper leukoencephalitis. *Acta Neuropathol* **110:** 369–382.

Hartung HP, Kieseier BC (2000). The role of matrix metalloproteinases in autoimmune damage to the central and peripheral nervous system. *J Neuroimmunol* **107:** 140–147.

Im HJ, Muddasani P, Natarajan V, Schmid TM, Block JA, David F, van Wijnen AJ, Loeser RF (2007). Basic fibroblast growth factor stimulates matrix metalloproteinase-13 via the molecular cross-talk between mitogen activated protein kinases and protein kinase Cδ pathways in human adult articular chondrocytes. *J Biol Chem* **282:** 11110–11121.

Jaworski DM (2000). Differential regulation of tissue inhibitor of metalloproteinase mRNA expression in response to intracranial injury. *Glia* **30:** 199–208.

Jelachich ML, Bramlage C, Lipton HL (1999). Differentiation of M1 myeloid precursor cells into macrophages results in binding and infection by Theiler's murine encephalomyelitis virus and apoptosis. *J Virol* **73:** 3227–3235.

Khasigov PZ, Podobed OV, Ktzoeva SA, Gatagonova TM, Grachev SV, Shishkin SS, Berezov TT (2001). Matrix Metalloproteinases of normal human tissues. *Biochemistry* **66:** 130–140.

Kieseier BC, Paul R, Koedel U, Seifert T, Clements JM, Gearing AJ, Pfister HW, Hartung HP (1999). Differential expression of matrix metalloproteinases in bacterial meningitis. *Brain* **122:** 1579–1587.

Leppert D, Lindberg RL, Kappos L, Leib SL (2001). Matrix metalloproteinases: multifunctional effectors of inflammation in multiple sclerosis and bacterial meningitis. *Brain Res Rev* **36:** 249–257.

Lindberg RLP, De Groot CJA, Montagne L, Freitag P, van der Valk P, Kappos L, Leppert D (2001). The expression profile of matrix metalloproteinases (MMPs) and their inhibitors (TIMPs) in lesions and normal appearing white matter of multiple sclerosis. *Brain* **124:** 1743–1753.

Lipton HL (1975). Theiler's virus infection in mice: an unusual biphasic disease process leading to demyelination. *Infect Immun* **11:** 1147–1155.

Lipton HL, Twaddle G, Jelachich ML (1995). The predominant virus antigen burden is present in macrophages in

Theiler's murine encephalomyelitis virus-induced demyelinating disease. *J Virol* **69:** 2525–2533.

Liuzzi GM, Latronico T, Fasabo A, Carlone G, Riccio P (2004). Interferon-beta inhibits the expression of metalloproteinases in rat glial culture implications for multiple sclerosis pathogenesis and treatment. *Mult Scler* **10:** 290–297.

Ma Z, Qin H, Benveniste EN (2001). Transcriptional suppression of matrix metalloproteinase-9 gene expression by IFN-gamma and IFN-beta: critical role of STAT-1alpha. *J Immunol* **167:** 5150–5159.

Markus S, Failing K, Baumgärtner W (2002). Increased expression of pro-inflammatory cytokines and lack of up-regulation of anti-inflammatory cytokines in early distemper CNS lesions. *J Neuroimmunol* **125:** 30–41.

Massova I, Kotra LP, Fridman R, Mobasery S (1998). Matrix metalloproteinases: structures, evolution, and diversification. *FASEB J* **12:** 1075–1095.

Matrisian LM (1990). Metalloproteinases and their inhibitors in matrix remodeling. *Trends Genet* **6:** 121–125.

McCarthy KD, de Vellis J (1980). Preparation of separate astroglial and oligodendroglial cell cultures from rat cerebral tissue. *J Cell Biol* **85:** 890–902.

McCawley LJ, Matrisian LM (2001). Matrix metalloproteinases: they're not just for matrix anymore. *Curr Opin Cell Biol* **13:** 534–540.

Miao Q, Baumgärtner W, Failing K, Alldinger S (2003). Phase-dependent expression of matrix metalloproteinases and their inhibitors in demyelinating canine distemper encephalitis. *Acta Neuropathol* **106:** 486–494.

Mun-Bryce S, Lukes A, Wallace J, Lukes-Marx M, Rosenberg GA (2002). Stromelysin-1 and gelatinase A are upregulated before TNF-[alpha] in LPS-stimulated neuroinflammation. *Brain Res* **933:** 42–49.

Neuhold LA, Killar L, Zhao W, Sung MLA, Warner L, Kulik J, Turner J, Wu W, Billinghurst C, Meijers T, Poole AR, Babij P, DeGennaro LJ (2001). Postnatal expression in hyaline cartilage of constitutively active human collagenase-3 (MMP-13) induces osteoarthritis in mice. *J Clin Invest* **107:** 35–44.

Oleszak EL, Chang JR, Friedman H, Katsetos CD, Platsoucas CD (2004). Theiler's virus infection: a model for multiple sclerosis. *Clin Microbiol Rev* **17:** 174–207.

Pagenstecher A, Stalder AK, Kincaid CL, Shapiro SD, Campbell IL (1998). Differential expression of matrix metalloproteinase and tissue inhibitor of matrix metalloproteinase genes in the mouse central nervous system in normal and inflammatory states. *Am J Pathol* **152:** 729–741.

Palma JP, Kim BS (2004). The scope and activation mechanisms of chemokine gene expression in primary astrocytes following infection with Theiler's virus. *J Neuroimmunol* **149:** 121–129.

Palma JP, Kwon D, Clipstone NA, Kim BS (2003). Infection with Theiler's murine encephalomyelitis virus directly induces proinflammatory cytokines in primary astrocytes via NF-kappaB activation: potential role for the initiation of demyelinating disease. *J Virol* **77:** 6322–6331.

Racaniello VR (2001). Picornaviridae: the viruses and their replication. In: *Field's virology.* Knipe, DM, Howley, PM, Griffin, DE, Lamb, RA, Martin, MA, Roizman, B, Strauss, SE (eds). *Philadelphia: Lippincott Williams & Wilkins* pp 685–722.

Ries C, Petrides PE (1995). Cytokine regulation of matrix metalloproteinase activity and its regulatory dysfunction in disease. *Biol Chem Hoppe-Seyler* **376:** 345–355.

Rosenberg GA (2001). Matrix metalloproteinases in multiple sclerosis: is it time for a treatment trial? *Ann Neurol* **50:** 431–433.

Rosenberg GA (2002). Matrix metalloproteinases in neuroinflammation. *Glia* **39:** 279–291.

Rosenberg GA (2005). Matrix metalloproteinases biomarkers in multiple sclerosis. *Lancet* **365:** 1291–1293.

Rosenberg GA, Estrada, EY, Dencoff, JE, Stetler-Stevenson, WG (1995). Tumor necrosis factor-alpha-induced gelatinase B causes delayed opening of the blood-brain barrier: an expanded therapeutic window. *Brain Res* **703:** 151–155.

Rozhon EJ, Kratochvil JD, Lipton HL (1983). Analysis of genetic variation in Theiler's virus persistent infection in the mouse central nervous system. *Virology* **128:** 16–32.

Rubio N, Capa L (1993). Differential IL-1 synthesis by astrocytes from Theiler's murine encephalomyelitis virus-susceptible and -resistant strains of mice. *Cell Immunol* **149:** 237–247.

Rubio N, Martin-Clemente B (1999). Theiler's murine encephalomyelitis virus infection induces early expression of c-fos in astrocytes. *Virology* **258:** 21–29.

Rubio N, Sanz-Rodriguez F, Lipton HL (2006). Theiler's virus induces the MIP-2 chemokine (CXCL2) in astrocytes from genetically susceptible but not from resistant mouse strains. *Cell Immunol* **239:** 31–40.

Rudolph-Owen LA, Hulboy DL, Wilson CL, Mudgett J, Matrisian M (1997). Coordinate expression of matrix metalloproteinase family members in the uterus of normal, matrilysin-deficient, and stromelysin-1-deficient mice. *Endocrinology* **138:** 4902–4911.

So EY, Kang MH, Kim BS (2006). Induction of chemokine and cytokine genes in astrocytes following infection with Theiler's murine encephalomyelitis virus is mediated by the Toll-like receptor 3. *Glia* **53:** 858–867.

Stamenkovic I (2003). Extracellular matrix remodeling: the role of matrix metalloproteinases. *J Pathol* **200:** 448–464.

Stohlman SA, Hinton DR (2001). Viral induced demyelination. *Brain Pathol* **11:** 92–106.

Teesalu T, Hinkkanen AE, Vaheri A (2001). Coordinated induction of extracellular proteolysis systems during experimental autoimmune encephalomyelitis in mice. *Am J Pathol* **159:** 2227–2237.

Theiler M (1934). Spontaneous encephalomyelitis of mice—a new virus disease. *Science* **80:** 122–123.

Thorns V, Walter GF, Thorns C (2003). Expression of MMP-2, MMP-7, MMP-9, MMP-10 and MMP-11 in human astrocytic and oligodendroglial gliomas. *Anticancer Res* **23:** 3937–3944.

Toft-Hansen H, Nuttall RK, Edwards DR, Owens T (2004). Key metalloproteinases are expressed by specific cell types in experimental autoimmune encephalomyelitis. *J Immunol* **173:** 5209–5218.

Tsunoda I, Iwasaki Y, Terunuma H, Sako K, Ohara Y (1996). A comparative study of acute and chronic diseases induced by two subgroups of Theiler's murine encephalomyelitis virus. *Acta Neuropathol* **91:** 595–602.

Ulrich R, Baumgärtner W, Gerhauser I, Seeliger F, Haist V, Deschl U, Alldinger S (2006). MMP-12, MMP-3, and TIMP-1 are markedly upregulated in chronic

demyelinating Theiler murine encephalomyelitis. *J Neuropathol Exp Neurol* **65:** 783–793.

Ulrich R, Gerhauser I, Seeliger F, Baumgärtner W, Alldinger S (2005). Matrix metalloproteinases and their inhibitors in the developing mouse brain and spinal cord: a reverse transcription quantitative polymerase chain reaction study. *Dev Neurosci* **27:** 408–418.

Vandesompele J, De Preter K, Pattyn F, Poppe B, Van Roy N, De Paepe A, Speleman F (2002). Accurate normalization of real-time quantitative RT-PCR data by geometric averaging of multiple internal control genes. Genome Biol, 3, published online: http://genomebiology.com/2002/3/7/research/0034.

Vos CM, van Haastert ES, de Groot CJ, van der Valk P, de Vries HE (2003). Matrix metalloproteinase-12 is expressed in phagocytotic macrophages in active multiple sclerosis lesions. *J Neuroimmunol* **138:** 106–114.

Welsh CJ, Tonks P, Borrow P, Nash AA (1990). Theiler's virus: an experimental model of virus-induced demyelination. *Autoimmunity* **6**: 105–112.

Woessner JF (1991). Matrix metalloproteinases and their inhibitors in connective tissue remodeling. *FASEB J* **5**: 2145–2153.

Yong VW, Krekoski CA, Forsyth PA, Bell R, Edwards DR (1998). Matrix metalloproteinases and diseases of the CNS. *Trends Neurosci* **21:** 75–80.

Zheng L, Calenoff MA, Dal Canto MC (2001). Astrocytes, not microglia, are the main cells responsible for viral persistence in Theiler's murine encephalomyelitis virus infection leading to demyelination. *J Neuroimmunol* **118:** 256–267.

Zhou J, Marten NW, Bergmann CC, Macklin WB, Hinton DR, Stohlman SA (2005). Expression of matrix metalloproteinases and their tissue inhibitor during viral encephalitis. *J Virol* **79:** 4764–4773.

Zhou J, Stohlman SA, Atkinson R, Hinton DR, Marten NW (2002). Matrix metalloproteinase expression correlates with virulence following neurotropic mouse hepatitis virus infection. *J Virol* **76:** 7374–7384.

Zoecklein LJ, Pavelko KD, Gamez J, Papke L, McGavern DB, Ure DR, Njenga MK, Johnson AJ, Nakane S, Rodriguez M (2003). Direct comparison of demyelinating disease induced by the Daniel's strain and BeAn strain of Theiler's murine encephalomyelitis virus. *Brain Pathol* **13:** 291–308.